Appl Magn Reson (2010) 37:123–136
DOI 10.1007/s00723-009-0051-1

Applied
Magnetic Resonance

Is Mn-Bound Substrate Water Protonated in the S_2 State of Photosystem II?

Ji-Hu Su · Johannes Messinger

Received: 15 June 2009 / Revised: 23 June 2009 / Published online: 13 November 2009

Abstract In spite of great progress in resolving the geometric structure of the water-splitting Mn_4O_xCa cluster in photosystem II, the binding sites and modes of the two substrate water molecules are still insufficiently characterized. While time-resolved membrane-inlet mass spectrometry measurements indicate that both substrate water molecules are bound to the oxygen-evolving complex (OEC) in the S_2 and S_3 states (Hendry and Wydrzynski in Biochemistry 41:13328–13334, 2002), it is not known (1) if they are both Mn-bound, (2) if they are terminal or bridging ligands, and (3) in what protonation state they are bound in the different oxidation states S_i ($i = 0, 1, 2, 3, 4$) of the OEC. By employing ^{17}O hyperfine sublevel correlation (HYSCORE) spectroscopy we recently demonstrated that in the S_2 state there is only one (type of) Mn-bound oxygen that is water exchangeable. We therefore tentatively identified this oxygen as one substrate 'water' molecule, and on the basis of the finding that it has a hyperfine interaction of about 10 MHz with the electron spin of the Mn_4O_xCa cluster, we suggest that it is bound as a Mn–O–Mn bridge within a bis-μ_2 oxo-bridged unit (Su et al. in J Am Chem Soc 130:786–787, 2008). Employing pulse electron paramagnetic resonance, $^1H/^2H$ Mims electron-nuclear double resonance and ^2H-HYSCORE spectroscopies together with $^1H/^2H$-exchange here, we test this hypothesis by probing the protonation state of this exchangeable oxygen. We conclude that this oxygen is fully deprotonated. This result is discussed in the light of earlier reports in the literature.

J.-H. Su · J. Messinger
Max-Planck-Institut für Bioanorganische Chemie, Mülheim an der Ruhr, Germany

J. Messinger (✉)
Department of Chemistry, Chemical Biological Center (KBC),
Umeå University, 90187 Umeå, Sweden
e-mail: Johannes.Messinger@chem.umu.se

1 Introduction

In oxygenic photosynthesis, light-driven water-oxidation to molecular oxygen is carried out by the oxygen-evolving complex (OEC) of photosystem II (PSII). PSII is a multi-subunit pigment–protein complex that is located in the thylakoid membranes of green plants, algae and cyanobacteria. It is the only known biological water-splitting catalyst, and it is responsible for converting the atmosphere of the Earth from being anaerobic (2.3 billion years ago) to containing $\sim$20% molecular oxygen [1]. The water-splitting catalyst within PSII is a Mn_4O_xCa cluster ($4 \leq x \leq 7$) of not yet fully resolved structure, where x signifies the number of oxygen bridges and terminal water-derived ligands [2]. The uncertainty in the structure originates from the fact that the analysis of PSII by X-ray crystallography is still hampered by limited resolution and by specific radiation damage to the Mn_4O_xCa cluster [3–5], and that extended X-ray absorption fine structure (EXAFS) spectroscopy cannot reveal the precise bridging pattern to Ca and the coordination of the surrounding ligands, including the two substrate water molecules. The surrounding protein microenvironment is important for tuning the energetics of water-splitting by allowing proton-coupled electron transfer and for regulating substrate access and product release [6–8]. One specifically important nearby protein side chain is tyrosine D_1-Tyr_{161} (or Tyr_Z), since it is responsible for the electron transfer between the Mn_4O_xCa cluster and $P_{680}^{\bullet+}$.

$P_{680}^{\bullet+}$ is formed after light absorption by the antenna complexes and excitation energy transfer to the reaction center of PSII. New data indicate that the primary charge separation occurs between a chlorophyll molecule termed Chl_{D1} and its neighboring $pheophytin_{D1}$ molecule [9]. Because of the strong coupling between the four reaction-center chlorophyll molecules [10], the radical is distributed over several pigments, including P_{D1} and P_{D2}. Driven by this photochemical reaction, the Mn_4O_xCa cluster undergoes a cycle composed of five distinct redox intermediates termed S_i states ($i = 0$–4) [11]. Molecular oxygen is released during the $S_3 \rightarrow [S_4] \rightarrow S_0$ transition. Under working conditions the S_0 state is the most reduced state of the Mn_4O_xCa cluster, but after sufficient dark-adaptation almost all centers are poised in the S_1 state. The S_2 and S_3 states are semi-stable and decay back to the S_1 state with $t_{1/2} = 3$–5 min (20°C, neutral pH), while the S_0 state is oxidized by Tyr_D^{ox} of the D2 protein [12] in a much slower reaction to the S_1 state [13]. The S_4 state is a so far untrapped transient intermediate.

In spite of the above-mentioned progress in structural determination of the OEC, it is still unknown when, where and how the substrate water molecules bind to the Mn_4O_xCa cluster during the S-state cycle. Because water is also required for the overall function of PSII, spectroscopic and functional studies of substrate binding need to employ either substrate analogs such as ammonia or methanol or isotope labeling ($^1H/^2H$, $^{16}O/^{17}O$, ^{18}O) [7, 14, 15]. Time-resolved membrane-inlet mass spectrometry experiments show that at least one substrate water molecule is bound in all S states, while both are bound in different chemical ways or environments in the S_2 and S_3 states [16–18]. Fourier-transform infrared (FTIR) spectroscopy measurements indicate that the hydrogen bond strength of one exchangeable, metal-(Mn, Ca)-bound water molecule gets more asymmetric during the $S_1 \rightarrow S_2$ transition [19, 20]. Similarly, nuclear magnetic resonance paramagnetic relaxation enhancement

(NMR-PRE or dispersion) measurements [21] were interpreted to show direct Mn-binding of at least one partially protonated water species in the S_2 state.

Further important tools for studying water-binding to Mn are (pulse) electron paramagnetic resonance (EPR) and electron-nuclear double resonance (ENDOR) spectroscopy. These techniques can detect the coupling of nuclear spins with the electron spin of $S = 1/2$ in the S_2 [22] and S_0 states [23–25] of the Mn_4O_xCa cluster. The strength of the coupling and whether it is isotropic or anisotropic can then be used to argue whether or not ^1H ($I = 1/2$), ^2H ($I = 1$) or ^{17}O ($I = 5/2$) are directly (protons via oxygen) bound to Mn.

The binding of water can be most directly probed by demonstrating the coupling of water-exchangeable oxygens to the electron spin of the Mn_4O_xCa cluster. Initially it was attempted to detect line broadenings of the S_2 multiline signal caused by the hyperfine coupling of ^{17}O [26]. However, the effects were rather small. Similarly, electron spin echo envelope modulation (ESEEM) studies were performed after $H_2^{16}O/H_2^{17}O$ exchange with varying results [27, 28]. Recently, we employed ^{17}O hyperfine sublevel correlation (HYSCORE) spectroscopy, which clearly revealed the coupling of one (type) of ^{17}O with the paramagnetic Mn_4O_xCa cluster (S_2 state). The determined coupling strength of 10–11 MHz is indicative of a water-exchangeable Mn–O–Mn bridge [29]. This site likely corresponds to an earlier reported low-frequency FTIR signal at 606 cm^{-1} that is sensitive to $H_2^{16}O/H_2^{18}O$-exchange and which was also assigned to a bridged oxo species [30, 31].

Somewhat more indirectly water binding can be probed via the observed changes in the hyperfine coupling of protons after $^1H/^2H$-exchange. These types of experiments can give vital information regarding the protonation state of Mn-bound substrate molecules/atoms. Therefore, X-band continuous-wave (CW) and Mims ENDOR and ESEEM spectroscopy in conjunction with $^1H_2O/^2H_2O$ (D_2O) exchange have been employed by several groups [32–38]. They all reveal several hyperfine interactions (HFI) in the order of 2–5 MHz between ^1H and the Mn_4O_xCa cluster (or correspondingly weaker once for ^2H). On the basis of these findings all but one study [34] conclude that at least one hydroxo or water is (or maybe) directly bound to Mn in the S_2 state.

Here, we employ multifrequency pulse EPR techniques to specifically address the question whether the exchangeable oxygen detected by ^{17}O HYSCORE is protonated.

2 Materials and Methods

2.1 PSII (BBY) Sample Preparation

Photosystem II membrane fragments (BBY) were isolated from spinach according to the method of Berthold and co-workers [39] with minor modifications. The oxygen-evolving activity of the PSII preparations at saturating light intensities was about 500 μmol (O_2) mg $(Chl)^{-1}$ h^{-1}.

2.2 $^1H_2O/^2H_2O$ (D_2O)-Substituted BBY Samples

The dark-adapted samples (S_1 state) were suspended in buffer containing 0.4 M sucrose, 25 mM 2-(N-morpholino)ethanesulfonic acid (MES)–NaOH (pH 6.1),

15 mM NaCl, and 3 mM $MgCl_2$. The samples were washed two times with ^2H_2O-enriched (>95%) buffer of identical composition. Finally, the samples were concentrated by 20 min centrifugation at 4°C in calibrated 4 mm X-band and 3 mm Q-band EPR tubes to a final concentration of 20–30 mg Chl/ml. The total incubation time in ^2H_2O was about 90 min. All samples contained ~3% (v/v) methanol.

2.3 Advancement of PSII Samples from S_1 to S_2 State

The PSII samples in the S_1 state were advanced to the S_2 state by 10–20 min continuous illumination at 200 K (dry ice/ethanol bath) using two 250 W halogen lamps, from which the infrared and ultraviolet contributions were largely removed by the following filters: 8 cm water, 2 cm $CuSO_4$ solution (5% w/v), *Schott KG 3* (2 mm) and *Schott GG 445* (2 mm). The final light intensity at the sample level was ~0.5 W/cm^2.

2.4 EPR Measurements

The measurements of X- and Q-band pulse EPR, τ-dependence/two-dimensional three-pulse (2D-3P) ESEEM, ^{2}H-HYSCORE and ^{1}H/^{2}H Mims ENDOR at 4.2 K were performed on Bruker ELEXSYS E-580 X- and Q-band pulse EPR spectrometers equipped with superXFT and superQFT bridges, respectively, and with Oxford-900 liquid helium cryostats and ITC-503 temperature controllers. The ^{1}H/^{2}H Mims ENDOR data were collected with Spec-Man software [40] as described in Refs. [41–43]. The corresponding pulse sequences and EPR settings are given in the figure legends. The microwave frequencies in the pulse X- and pulse Q-band measurements were 9.71 and 33.9 GHz, respectively.

3 Results

3.1 X-band Pulse EPR Measurements in the S_2 State

Figure 1 shows the X-band light-minus-dark S_2 state electron spin echo (ESE)-detected field-swept difference spectrum of our concentrated (20–30 mg Chl/ml) spinach PSII membrane sample after washing into ^2H_2O. The hyperfine lines of the S_2 multiline signal can be discerned as steps. This shows that the S_2 state can be generated in this sample. The vertical bar and the arrow mark the field positions where the ESEEM/HYSCORE and ^{1}H/^{2}H ENDOR measurements were performed (see below).

3.2 X- and Q-Band ^{1}H/^{2}H Mims ENDOR

It was reported previously in the literature that the ^{2}H signal originating from the exchangeable ^{2}H can be detected by the X-band ^{2}H CW and Mims ENDOR, and in two-pulse and three-pulse (2P/3P) ESEEM experiments (see Sect. 1). Here we employ ^{1}H/^{2}H Mims ENDOR, a sensitive technique to probe at X- and Q-band

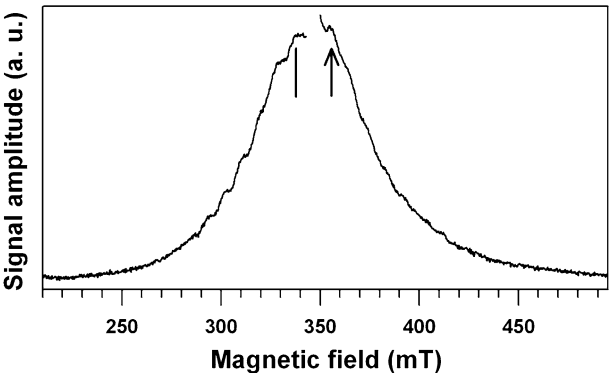

Fig. 1 Light-minus-dark ESE-detected field-swept X-band EPR spectrum of the S_2 state in PSII membrane fragments at 4.2 K. The sample was highly enriched (>95%) in ^2H_2O and had a Chl concentration of about 20–30 mg/ml. The used pulse sequence is a $\pi/2$–τ–π pulse, where $\pi/2 = 12$ ns, $\tau = 128$ ns, and shots repetition time (SRT) = 5 ms with microwave frequency of 9.70 GHz. The displayed signal represents the average of four scans. The absorption of the $Tyr_D^{\bullet}$ radical was removed for the presentation. The *vertical bar* and the *arrow* indicate the field positions where the Mims ENDOR and ESEEM/HYSCORE were measured in Figs. 2, 3 and 4, respectively

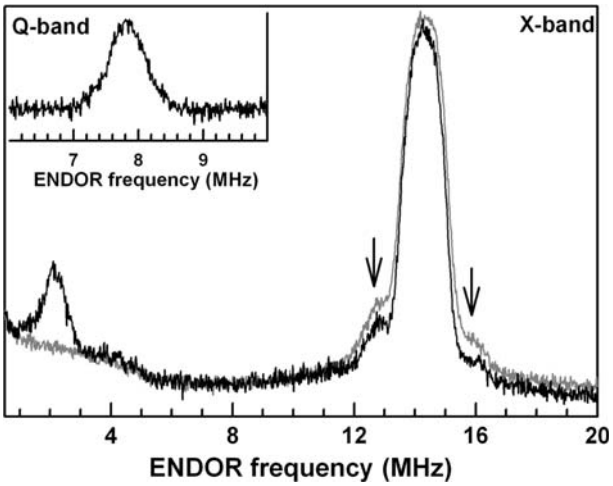

Fig. 2 $^1H/^2H$ Mims ENDOR of concentrated PSII membranes from spinach suspended either in ^2H_2O-enriched (*black*) or in ^1H_2O-buffer (*gray*). The data were recorded with a pulse sequence $\pi/2$–τ–$\pi/2$–t_{rf}–$\pi/2$–τ-echo, where $\pi/2 = 200$ ns, $\tau = 420$ ns, the length of rf pulse t_{rf} was 25 µs in both X- and Q-band measurements. The Larmor frequencies of ^2H in X-band ($B_0 = 335$ mT, 9.70 GHz) and Q-band ($B_0 = 1220$ mT, 33.93 GHz) are 2.19 and 7.974 MHz, respectively. For ^1H, it is 14.26 MHz ($B_0 = 335$ mT) in X-band. The *inset* spectrum was measured at Q-band (^2H_2O-enriched sample). The *arrows* indicate the positions of ^1H-signals from exchangeable protons

frequencies directly the weak HFI of highly concentrated BBY samples in buffer either enriched in ^1H_2O or ^2H_2O. The obtained results are displayed in Fig. 2. In the ^1H_2O sample, the ^1H signal is centered at X-band at the ^1H Larmor frequency of 14.26 MHz ($B_0 = 335$ mT). Additionally two weak shoulders (see the arrows) were observed (gray spectrum in Fig. 2). No signal above background was detected in the

region of 0–10 MHz. After the $^{1}H_2O/^{2}H_2O$ substitution, the ^{2}H signal was detected at a radio frequency (rf) position of around 2.19 MHz (the ^{2}H Larmor frequency at $B_0 = 335$ mT) and a width of $\sim$1.5 MHz (black spectrum in Fig. 2). This signal was broadened without revealing a clear splitting, which in principle would be centered at ν_{2H} (2.19 MHz) with a splitting distance of A, i.e., $\nu_{2H} \pm A/2$. The appearance of the new signal after $^{1}H_2O/^{2}H_2O$ substitution demonstrates, in agreement with the previous reports, that there are water-exchangeable protons in the vicinity of Mn in the S_2 state. Additionally, also the signal at 14.26 MHz is still observed, which originates from non-exchangeable protons that couple with the Mn_4O_xCa cluster and other underlying EPR signals like $Tyr_D^{\bullet}$. Since we know from time-resolved membrane-inlet mass spectrometry that substrate water exchanges completely within a few seconds [16, 44], the latter signal cannot originate from substrate water protons.

To improve the resolution of the ^{2}H signal, Mims ENDOR was measured also at Q-band frequency (34 GHz). While the signal moved as expected to the ^{2}H Larmor frequency at Q-band of 7.9 MHz, the signal remained unresolved with a width of $\sim$1.5 MHz despite trying various different τ values to avoid the blind-spot behavior in Mims ENDOR (see Sect. 3.3).

For the same element, it is known that the HFIs of different isotopes have a good proportion to the corresponding nuclear magnetogyric ratio, i.e., g_{1H}/g_{2H}, with $g_{1H} = 5.5856948$ and $g_{2H} = 0.8574388288$. Therefore, a scrutinized inspection was conducted on the difference between the ^{1}H X-band Mims ENDOR obtained in the $^{1}H_2O$- and $^{2}H_2O$-enriched samples. Figure 2 shows that some exchangeable ^{1}H signals splitting with HFI of $A_{1H} = 2.5$–4 MHz disappeared after the $^{2}H_2O$ substitute (see arrows). With respect to the ratio $g_{1H}/g_{2H} = 6.5144$, these exchanged ^{1}H signals give rise to the corresponding ^{2}H signals with the HFI of $A_{2H} = 0.4$–0.6 MHz, which are equal to approximately half of the width (1.5 MHz) of the broad ^{2}H signal (the two black spectra in Fig. 2). These data demonstrated that the HFIs between the ^{2}H and the Mn_4O_xCa cluster are fairly weak (see also Sect. 4). Thus, 3P-ESEEM and ^{2}H-HYSCORE were used in the following measurements to further characterize the nature of this coupling.

3.3 X-band 2D-3P ESEEM in the $^{2}H_2O$-Enriched Samples

In practice it is often found that there is a similar blind-spot behavior in 3P-ESEEM and HYSCORE experiments. At blind-spots no nuclear coherence is generated by the microwave pulses. To avoid these conditions in subsequent HYSCORE experiments, the τ-dependence/2D-3P ESEEM (2D-3P ESEEM) was recorded for a $^{2}H_2O$-enriched sample at the magnetic field of $B_0 = 355$ mT. The data obtained are displayed in Fig. 3. They display both a weak ^{1}H signal (because of high $^{2}H_2O$ enrichment) and a strong ^{2}H signal centered at 15.1 and 2.3 MHz, respectively. Both signals show the discussed above blind-spot behavior with oscillating signal intensity, when τ increased from 118 to 800 ns. Figure 3 also shows weak ^{14}N signals at 3–8 MHz. The origin of the ^{14}N signals is still

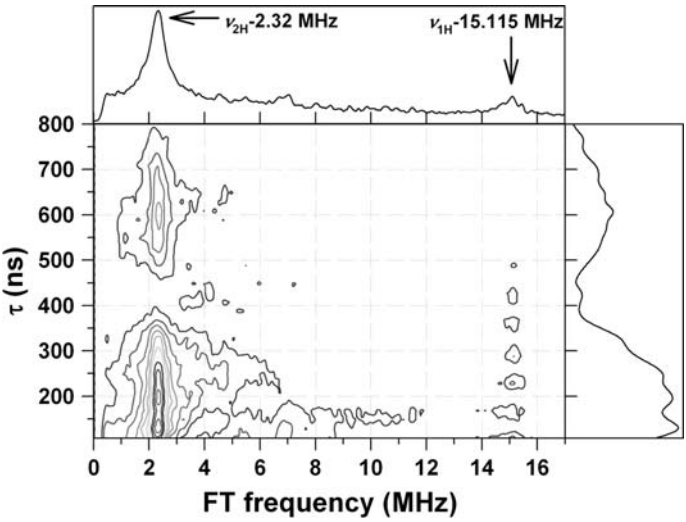

Fig. 3 2D-3P ESEEM of concentrated PSII membranes from spinach suspended in ^2H_2O-enriched buffer. The spectra were recorded with the pulse sequence $\pi/2$–τ–$\pi/2$–T–$\pi/2$–τ-echo, where $\pi/2 = 24$ ns and τ was varied from 108 to 888 ns in 20 ns steps. T was varied from 48 to 6192 ns in 24 ns steps. Four-phase cycling with 50 shots/point and a shot repetition time of 5 ms was employed. The magnetic field was set to $B_0 = 355$ mT. The Larmor frequencies of ^1H and ^2H are 15.115 and 2.32 MHz, respectively. After Fourier transformation, the *projections on the top* and *on the right* show the 1D spectrum in the frequency domain, and the oscillation of the signal amplitude as a function of τ, respectively

not clear, but it is known that the Mn_4O_xCa cluster has one direct histidine ligand [45].

3.4 X-band ^2H-HYSCORE in the ^2H_2O-Enriched Samples

In HYSCORE measurements, signals may be resolved in two separate quadrants based on the relation of $|\nu| > |A/2|$ and $|\nu| < |A/2|$, respectively, where ν is the Larmor frequency of the nucleus under investigation and A is the HFI between the nuclear spin and the electron spin (of Mn_4O_xCa cluster). Figure 4 shows only the $(++)$ quadrant of our ^2H-HYSCORE spectrum measured with $\tau = 252$ ns, since no signal was detectable in the $(-+)$ quadrant. The absence of a single in the $(-+)$ quadrant is in sharp contrast to our recent ^{17}O HYSCORE data and shows that there are no strong HFIs between ^2H and the Mn_4O_xCa cluster in the S_2 state. In the $(++)$ quadrant (Fig. 4), a strong ^2H signal is seen that is centered at the ^2H Larmor frequency of 2.32 MHz at $B_0 = 355$ mT. The broad line shape indicates the presence of a weak, unresolved HFI. Similar results were observed in other HYSCORE measurements performed at several other τ values (128, 156, 188, 216, 300, and 616 ns). All these results indicated that the HFI between the ^2H and the Mn_4O_xCa cluster is too weak to be resolved by HYSCORE. Clearly no strong or intermediate HFI between exchangeable protons and the Mn_4O_xCa cluster are present.

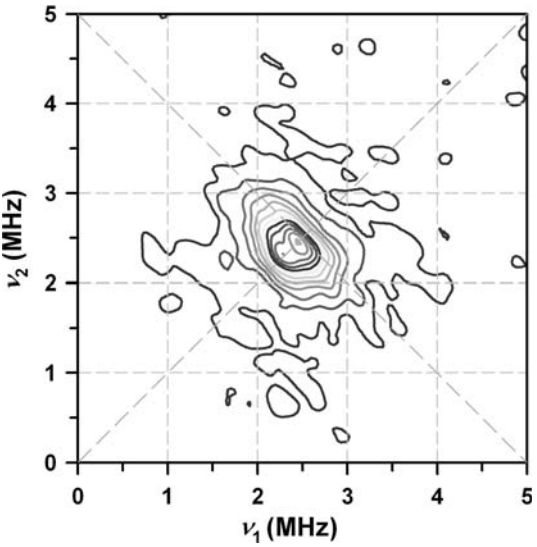

Fig. 4 X-band ^{2}H-HYSCORE spectrum of concentrated PSII membranes from spinach suspended in ^2H_2O-enriched buffer. The spectrum was recorded with a pulse sequence $\pi/2$–τ–$\pi/2$–t_1–π–t_2–$\pi/2$–τ-echo with $\pi/2 = 24$ ns. The times t_1 and t_2 were varied from 60 to 6,720 ns in 24 ns steps. Four-phase cycling with 50 shots/point and a shot repetition time of 5 ms was employed. Other parameters: $B_0 = 355$ mT, $\tau = 256$ ns and the microwave frequency was 9.70 GHz

4 Discussion

4.1 Protonation State of Bound Substrate Water in the S_2 State

In our previous study, a 10-MHz HFI between one bulk water-exchangeable oxygen with the electron spin on the Mn_4O_xCa cluster was detected in the S_2 state of PSII by the ^{17}O-HYSCORE. This showed that in the S_2 state there is very likely only one (type of) Mn-ligated oxygen that can be readily exchanged with bulk water (note of caution: in EPR the absence of a signal is no absolute proof for the absence of an interaction). In the present study, we endeavored to probe the protonation state of this bound 'water' in the S_2 state by employing isotope labeling with ^2H_2O and several pulse EPR techniques at X- and Q-band frequencies. These techniques are sensitive to HFIs between ^{1}H or ^{2}H and the paramagnetic Mn_4O_xCa cluster. In our report we focus on ^{2}H couplings, since they represent bulk water exchangeable protons—a minimal requirement for protons of substrate water.

The coupling strength of a deuterium bound to this exchangeable oxygen can be estimated on the basis of simple considerations as follows: it is well established that the Mn–O distance is typically 1.8–2 Å in a bridge, and $\sim$2.2 Å to a terminal water ligand [46–48]. The O–^{1}H and O–^{2}H distances are $\sim$1 Å. Therefore, the maximal distance between the ^{1}H/^{2}H and the Mn ion(s) via the oxygen is 2.8–3.2 Å. Since the Fermi contact interaction is proportional to the g-factors of ^{17}O (0.758) and ^{2}H (0.857), and inversely proportional to the cubed through-bond distance (d^3), a minimal isotropic hyperfine interaction A_{2H} of about 3 MHz can be roughly estimated based on:

$$A_{2H} = A_{17O} \times \frac{d^3_{(170-Mn)}}{d^3_{(2H-Mn)}} \times \frac{g_{2H}}{g_{17O}}$$

In contrast to this expectation, all results obtained in this study for the ^2H_2O-enriched samples show just a broadened ^2H signal of $\sim$1.5 MHz width without resolved splitting according to $\nu_{2H} \pm A_{2H}/2$. This indicates that the coupling between the deuterons and the electron spin on the Mn_4O_xCa cluster is rather weak. The strength of this HFI can be estimated indirectly from the observation of Fig. 2 that in the Mims ENDOR, the occurrence of the ^2H signal after $^1H/^2H$ exchange leads to a small decrease of the ^1H signal (see arrows in Fig. 2) that have a HFI of $A_{1H} = 2.5$–4 MHz. For an element, the HFIs of different isotopes are, to a good approximation, proportional to their corresponding nuclear magnetogyric ratios (i.e., $g_{1H} = 5.5856948$ and $g_{2H} = 0.8574388288$). Due to $g_{1H}/g_{2H} = 6.5144$, these exchanged ^1H signals give rise to the corresponding ^2H signals with the HFI of $A_{2H} = 0.4$–0.6 MHz, which are 30–40% of the full width (1.5 MHz) of the observed ^2H signal.

We therefore conclude that in agreement with our previous proposal the water-exchangeable oxygen of the Mn_4O_xCa cluster represents one fully deprotonated substrate 'water' that is likely bonded as a bridge in a Mn-bis μ_2-oxo-Mn unit of the Mn_4O_xCa cluster in the S_2 state. However, binding as mono-μ-oxo or in a Mn-μ_3-oxo-μ_2-oxo-Mn unit or even binding as terminal Mn=O may not be ruled out entirely on the basis of just these measurements without further model studies and detailed theoretical calculations. It is noted that a terminal Mn=O is disfavored by X-ray absorption near-edge structure experiments on model complexes [49].

Our previous ^{17}O data and the current $^1H/^2H$ results do not provide evidence for a second Mn-bound water molecule in the S_2 state. Therefore, if a second substrate water molecule is bound in the OEC in the S_2 state, as suggested by time-resolved membrane-inlet mass spectrometry, this water is likely coordinated to Ca^{2+} or to protein ligands. On the other hand, our data are also consistent with a recent proposal by Siegbahn [50] that suggests that the second water molecule binds during the structural rearrangement that occurs in the $S_2 \rightarrow S_3$ transition.

The above conclusions are in agreement with two previous findings. Dismukes and coworkers [34] reported three weak hyperfine interactions of 4.5, 2.9 and 1.5 MHz and a very weak isotropic coupling of about 0.5 MHz as revealed by ^1H ENDOR spectroscopy. On the basis of a spin-coupled point-pair model Dismukes et al. [34] estimated that the minimal distance to the nearest exchangeable ^1H is 3.65 Å. On this basis it was concluded that the Mn_4O_xCa cluster is basically 'dry' with only weak H bonds to oxo-bridges, and that all water ligands directly bound to Mn must be fully deprotonated. A possible role of Ca in water binding was discussed [34]. However, on the basis of similar data and using a more complex theoretical modeling Fiege et al. [35] did not fully exclude direct water-binding to Mn.

A second line of support comes from a pioneering low-frequency FTIR study by Babcock and coworkers [30]. In this study, a 606 cm^{-1} mode was found in the S_2 state that corresponds to a mode at 625 cm^{-1} in the S_1 state. This mode was clearly downshifted after exchange with $H_2^{18}O$ to 596 cm^{-1}. This exchange was complete in less than 30 min. By comparison to existing data on model compounds this mode was concluded to most likely arise from the exchange of only one oxo within a Mn–bis-μ_2-oxo–Mn unit or possibly within a Mn–μ_3-oxo-μ_2-oxo–Mn unit. The latter suggestion might be able to explain why only one of the oxos is exchangeable. Furthermore, Babcock et al. [30] showed that the frequency of this oxo is upshifted

to 618 cm^{-1} by Ca^{2+}/Sr^{2+} exchange, but that it was unaffected by $^{40}Ca^{2+}/^{44}Ca^{2+}$ exchange. This was taken as evidence that Ca^{2+} is not directly involved in binding of this oxo, but that the exchange of Ca^{2+} against Sr^{2+} affects the binding of this oxo indirectly, for example, via structural changes of the cluster or its protein microenvironment. This finding will be important later on in the discussion on substrate water exchange rates.

However, there are also apparent conflicts with several recent reports that propose the binding of protonated water to the Mn_4O_xCa cluster in the S_2 state. These concerns are addressed in the following sections.

^{1}H ENDOR studies by Kawamori and coworkers [32] and by Yamada et al. [38] report several ^{1}H signals at frequencies of 2–4 MHz that are partly exchangeable against bulk ^2H_2O at relatively slow time scales (3–24 h). Point dipole approximations yield relatively short distances of about 2.7–3.3 Å. This was taken as evidence for the binding of protonated substrate water to Mn. Similarly Britt and coworkers [36] using $^1H/^2H$ ESEEM spectroscopy reported several classes of exchangeable deuterons. The most interesting one was concluded to comprise two ^{2}H with an isotropic coupling of 0.45 MHz and an anisotropic coupling of 0.64 MHz. Again a point dipole approximation was employed to estimate a distance of 2.67 Å, which together with the isotropic coupling was taken as evidence for the binding of one H_2O or two OH^- to Mn. Since ^{55}Mn ENDOR data reveal that the electron spin of the S_2 state is distributed over all four Mn ions [51], the dipole approximation is likely a too simple model and therefore thus calculated distances cannot be taken as reliable indicators for the binding of protonated water to Mn. It should be noted that the magnitude of the reported ^{1}H and ^{2}H couplings compares well with the estimated ranges in this report.

Nugent, Evans and coworkers [27] performed two ^{17}O ESEEM studies. In the first study [27], they concluded that the Mn_4O_xCa cluster does not contain any exchangeable oxygen since no ^{17}O HFI was found. In the second study [28], a ^{17}O coupling was reported for the central part of the S_2 multiline signal and the binding of water (not hydroxyl) to a quasi-axial Mn^{III} center was proposed. However, the reported couplings are not consistent with our later ^{17}O HYSCORE study [29].

With the help of FTIR spectroscopy at higher frequencies Noguchi and Sugiura [20] found two modes in the S_2–S_1 difference spectrum in the weakly H-bonded OH region, which appeared at 3617 and 3588 cm^{-1}. These modes were sensitive to $^2H_2O/^1H_2O$ exchange and to $H_2^{16}O/H_2^{18}O$ substitution, and thereby provide strong evidence for a water molecule that changes its hydrogen bond strength upon *S* state turnover. It was suggested that this water molecule is coupled to metal (Ca or Mn) [19], however, no strong evidence, except for the *S*-state dependence, was presented for this. It is therefore possible, that this water molecule is not Mn-bound, but either bound to Ca or to an amino acid in the vicinity of the Mn_4O_xCa cluster. Both latter options would be consistent with our findings.

Kimura et al. [31] determined the full *S* state dependence of the low-frequency FTIR signals. In this detailed study three classes of oxygen and hydrogen interactions were observed. Class one was only sensitive to $^{16}O/^{18}O$ exchange. This class corresponds to the 606 cm^{-1} mode of Chu et al. [30] discussed above and was also assigned to a Mn–O–Mn moiety. The second class was only sensitive to $^1H/^2H$

exchange and was assigned to exchangeable hydrogens of side chains or of the protein backbone. The class III signals were sensitive to both $^{16}O/^{18}O$ and $^{1}H/^{2}H$ exchange. These signals therefore belong very likely to water molecules or hydroxide ions in the vicinity of the Mn_4O_xCa cluster. The authors [30] favor direct binding of this potential substrate 'water' to Mn. It seems likely that the same moiety gives rise to the class III signals and to the high frequency once observed by Noguchi and Sugiura [20]. However, it appears that the suggestion of direct Mn binding is largely based on the cited previous suggestions by ESEEM and ENDOR. Indeed, the authors [30] do not exclude water/hydroxide binding to Ca or H-bridging to a Mn–O–Mn bridge.

NMR-PRE experiments originally performed by Wydrzynski et al. [52] and later by Sharp and coworkers [21] show that the relaxation rate of the protons in the bulk water is dependent on the oxidation state of the Mn_4O_xCa cluster. This suggests that there is at least one bound water or hydroxo directly coordinated to Mn, so that this relaxation enhancement by the paramagnetic Mn_4O_xCa cluster can be transmitted via exchange reactions to the bulk phase. However, the theory for this effect is complex and straightforward conclusions cannot be made on the basis of the current data and their analysis.

We therefore conclude that there is no, to our knowledge, compelling evidence in the literature that demonstrates binding of water or hydroxide to Mn in the S_2 state of PSII. In contrast, three independent experiments strongly favor the conclusion that there is one exchangeable oxo group in the S_2 state, which therefore likely represents one of the two substrate water molecules. Substrate water exchange experiments have demonstrated that the two substrate molecules bind in different chemical environments because they exchange in the S_2 and S_3 states with different rates and activation energies [16, 44]. Accordingly, the two substrate water molecules were denoted as fast-exchanging (W_f) and slow-exchanging (W_s) [53]. It is now interesting to speculate if the proposed μ_2-oxo-bridge corresponds to W_f or W_s.

Since the other substrate molecule (not detectable in this study) is either bound to Ca or the protein, it is very likely that the exchangeable μ_2-oxo-bridge can be identified with W_s. This assignment may be thought to be in conflict with the finding that the slow phase of water exchange is more strongly affected by Ca^{2+}/Sr^{2+} exchange than the fast phase [54]. First, one has to note that the fast phase of exchange was only resolved in these experiments in the S_3 state and not in the S_2 state. This is important since EXAFS and other experiments indicate a significant structural change between the S_2 and S_3 state within the Mn_4O_xCa cluster [55, 56]. Second, as summarized above, Chu et al. [30] showed that the FTIR mode of the oxo-bridge is sensitive to Ca^{2+}/Sr^{2+} exchange, without direct binding of the oxo to Ca. This observed frequency shift demonstrates the sensitivity of the proposed W_s to Ca^{2+}/Sr^{2+} exchange. The smaller effect on the fast phase may then be explained by the assumption that this exchange rate is not limited by binding to Ca^{2+}/Sr^{2+}, but by other factors such as, for example, diffusion through the protein to the active site. This would be consistent with the smaller activation energy that is coupled with this exchange compared to the slow exchange rate. Furthermore, our assignment of W_s is consistent with a theoretical study by Siegbahn and coworkers [57]. By employing density functional theory calculations they estimated the energetic

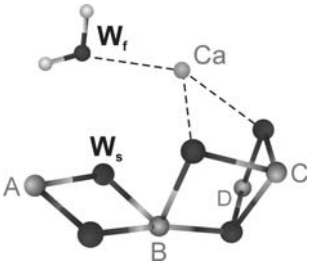

Fig. 5 Proposed substrate 'water' binding modes and sites at the S_2 state of the Mn_4O_xCa. W_s and W_f represent the slow- and the fast-exchanging substrate 'water' molecules as determined by time-resolved membrane-inlet mass spectrometry [16, 44]. The four Mn ions are denoted as *A*, *B*, *C*, *D*, while the oxygen ions are represented by *dark spheres*. The structural model employed is based on single-crystal EXAFS spectroscopy [2] and theoretical calculations [61]

barriers for terminal water or hydroxo versus oxo-bridges within a bis-μ_2-oxo-bridged Mn dimer. While a direct comparison of this simple model to the exchange processes within the OEC is rather complicated, the data are best in agreement with W_s being a bridging oxygen, while the exchange of W_f is limited by diffusion through the protein. However, another theoretical study implies that within the PSII complex water bound to Ca^{2+} exchanges, in contrast to what is known from solutions, more slowly than a terminal Mn(IV)=O species [58].

On the basis of this discussion a picture of water binding in the S_2 state arises, in which W_s is a fully deprotonated substrate water that is bound directly to the Mn, probably in form of a μ_2-oxo-bridge between Mn_A and Mn_B, while W_f probably corresponds to the water observed by Noguchi and Sugiura [20] and is therefore fully protonated and either bound to Ca or to a nearby amino acid. This conclusion is illustrated in Fig. 5 on the basis of a recent model of the Mn_4O_xCa cluster (however, if the calculations by Batista and coworkers [58] are correct, then the assignment of W_f and W_s would have to be reversed). The reason why only one oxo-bridge can be exchanged, and why this rate is faster than expected on the basis of some recent mass spectrometry-based experiments [59, 60] is closely coupled to the not yet fully resolved structure of the OEC and therefore remains to be established in future studies.

Acknowledgments All experiments were performed at the Max-Planck-Institute for Bioinorganic Chemistry, Mülheim an der Ruhr. Financial supported was provided by the Deutsche Forschungsgemeinschaft (Me1629/2-4), the Max Planck Gesellschaft and the Wallenberg foundation (to J.M.).

References

1. W. Lubitz, E.J. Reijerse, J. Messinger, Energy Environ. Sci. **1**, 15–31 (2008)
2. J. Yano, J. Kern, K. Sauer, M.J. Latimer, Y. Pushkar, J. Biesiadka, B. Loll, W. Saenger, J. Messinger, A. Zouni, V.K. Yachandra, Science **314**, 821–825 (2006)

3. K.N. Ferreira, T.M. Iverson, K. Maghlaoui, J. Barber, S. Iwata, Science **303**, 1831–1838 (2004)
4. J. Yano, J. Kern, K.D. Irrgang, M.J. Latimer, U. Bergmann, P. Glatzel, Y. Pushkar, J. Biesiadka, B. Loll, K. Sauer, J. Messinger, A. Zouni, V.K. Yachandra, Proc. Natl. Acad. Sci. USA **102**, 12047–12052 (2005)
5. A. Guskov, J. Kern, A. Gabdulkhakov, M. Broser, A. Zouni, W. Saenger, Nat. Struct. Biol. Mol. Biol. **16**, 334–342 (2009)
6. T. Wydrzynski, W. Hillier, J. Messinger, Physiol. Plantarum **96**, 342–350 (1996)
7. W. Hillier, J. Messinger, in *Photosystem II. The Light-Driven Water: Plastoquinone Oxidoreductase*, vol. 22, ed. by T. Wydrzynski, K. Satoh (Springer, Dordrecht, 2005) pp. 567–608
8. G. Renger, T. Renger, Photosynth. Res. **98**, 53–80 (2008)
9. A.R. Holzwarth, M.G. Müller, M. Reus, M. Nowaczyk, J. Sander, M. Rögner, Proc. Natl. Acad. Sci. USA **103**, 6895–6900 (2006)
10. J.P. Dekker, R. Van Grondelle, Photosynth. Res. **63**, 195–208 (2000)
11. B. Kok, B. Forbush, M. McGloin, Photochem. Photobiol. **11**, 457–476 (1970)
12. S. Styring, A.W. Rutherford, Biochemistry **26**, 2401–2405 (1987)
13. S. Isgandarova, G. Renger, J. Messinger, Biochemistry **42**, 8929–8938 (2003)
14. R.J. Debus, BBA Bioenergetics **1102**, 269–352 (1992)
15. B. Nöring, D. Shevela, G. Renger, J. Messinger, Photosynth. Res. **98**, 251–260 (2008)
16. J. Messinger, M. Badger, T. Wydrzynski, Proc. Natl. Acad. Sci. USA **92**, 3209–3213 (1995)
17. G. Hendry, T. Wydrzynski, Biochemistry **41**, 13328–13334 (2002)
18. W. Hillier, T. Wydrzynski, Biochim. Biophys. Acta Bioenerg. **252**, 306–317 (2008)
19. T. Noguchi, Coord. Chem. Rev. **252**, 336–346 (2008)
20. T. Noguchi, M. Sugiura, Biochemistry **41**, 15706–15712 (2002)
21. P.R. Sharp, in *Manganese Redox Enzymes*, vol. 177–196, ed. by V.L. Pecoraro (VCH Publishers, New York, 1992)
22. G.C. Dismukes, Y. Siderer, Proc. Natl. Acad. Sci. USA **78**, 274–278 (1981)
23. J. Messinger, J.H. Robblee, W.O. Yu, K. Sauer, V.K. Yachandra, M.P. Klein, J. Am. Chem. Soc. **119**, 11349–11350 (1997)
24. J. Messinger, J.H.A. Nugent, M.C.W. Evans, Biochemistry **36**, 11055–11060 (1997)
25. K.A. Åhrling, S. Peterson, S. Styring, Biochemistry **36**, 13148–13152 (1997)
26. Ö. Hansson, L.-E. Andréasson, T. Vänngård, FEBS Lett. **195**, 151–154 (1986)
27. S. Turconi, D.J. MacLachlan, P.J. Bratt, J.H.A. Nugent, M.C.W. Evans, Biochemistry **36**, 879–885 (1997)
28. M.C.W. Evans, J.H.A. Nugent, R.J. Ball, I. Muhiuddin, R.J. Pace, Biochemistry **43**, 989–994 (2004)
29. J.H. Su, W. Lubitz, J. Messinger, J. Am. Chem. Soc. **130**, 786–787 (2008)
30. H.-A. Chu, H. Sackett, G.T. Babcock, Biochemistry **39**, 14371–14376 (2000)
31. Y. Kimura, A. Ishii, T. Yamanari, T.A. Ono, Biochemistry **44**, 7613–7622 (2005)
32. A. Kawamori, T. Inai, T. Ono, Y. Inoue, FEBS Lett. **254**, 219–223 (1989)
35. W. Lubitz, W. Zweygart, G. Renger, T. Weyermüller, K. Wieghardt, Photosynth. Res. **34**, 144 (1992)
34. X.-S. Tang, M. Sivaraja, G.C. Dismukes, J. Am. Chem. Soc. **115**, 2382–2389 (1993)
35. R. Fiege, W. Zweygart, R. Bittl, N. Adir, G. Renger, W. Lubitz, Photosynth. Res. **42**, 227–244 (1996)
36. C.P. Aznar, R.D. Britt, Philos. Trans. R. Soc Lond. B **357**, 1359–1365 (2002)
37. R.D. Britt, K.A. Campbell, J.M. Peloquin, M.L. Gilchrist, C.P. Aznar, M.M. Dicus, J. Robblee, J. Messinger, Biochim. Biophys. Acta Bioenerg. **1655**, 158–171 (2004)
38. H. Yamada, H. Mino, S. Itoh, Biochim. Biophys. Acta Bioenerg. **1767**, 197–203 (2007)
39. D.A. Berthold, G.T. Babcock, C.F. Yocum, FEBS Lett. **134**, 231–234 (1981)
40. B. Epel, I. Gromov, S. Stoll, A. Schweiger, D. Goldfarb, Concepts Mag. Reson. B Magn. Reson. Eng. **26B**, 36–45 (2005)
41. L. Kulik, B. Epel, J. Messinger, W. Lubitz, Photosynth. Res. **84**, 347–353 (2005)
42. L.V. Kulik, B. Epel, W. Lubitz, J. Messinger, J. Am. Chem. Soc. **127**, 2392–2393 (2005)
43. L.V. Kulik, B. Epel, W. Lubitz, J. Messinger, Concepts Magn. Reson. **129**, 13421–13435 (2007)
44. W. Hillier, T. Wydrzynski, Biochemistry **39**, 4399–4405 (2000)
45. X.S. Tang, B.A. Diner, B.S. Larsen, M.L. Gilchrist, G.A. Lorigan, R.D. Britt, Proc. Natl. Acad. Sci. USA **91**, 704–708 (1994)
46. V.K. Yachandra, K. Sauer, M.P. Klein, Chem. Rev. **96**, 2927–2950 (1996)
47. V.J. DeRose, I. Mukerji, M.J. Latimer, V.K. Yachandra, K. Sauer, M.P. Klein, J. Am. Chem. Soc. **116**, 5239–5249 (1994)

48. V.K. Yachandra, V.J. DeRose, M.J. Latimer, I. Mukerji, K. Sauer, M.P. Klein, Science **260**, 675–679 (1993)
49. T.C. Weng, W.Y. Hsieh, E.S. Uffelman, S.W. Gordon-Wylie, T.J. Collins, V.L. Pecoraro, J.E. Penner-Hahn, J. Am. Chem. Soc. **126**, 8070–8071 (2004)
50. P.E.M. Siegbahn, Chem. Eur. J. **14**, 8290–8302 (2008)
51. J.M. Peloquin, K.A. Campbell, D.W. Randall, M.A. Evanchik, V.L. Pecoraro, W.H. Armstrong, R.D. Britt, J. Am. Chem. Soc. **122**, 10926–10942 (2000)
52. T. Wydrzynski, N. Zumbulyadis, P.G. Schmidt, H.S. Gutowsky, Govindjee, Proc. Natl. Acad. Sci. USA **73**, 1196–1198 (1976)
53. J. Messinger, Phys. Chem. Chem. Phys. **6**, 4764–4771 (2004)
54. G. Hendry, T. Wydrzynski, Biochemistry **42**, 6209–6217 (2003)
55. W. Liang, T.A. Roelofs, R.M. Cinco, A. Rompel, M.J. Latimer, W.O. Yu, K. Sauer, M.P. Klein, V.K. Yachandra, J. Am. Chem. Soc. **122**, 3399–3412 (2000)
56. M. Haumann, C. Müller, P. Liebisch, L. Iuzzolino, J. Dittmer, M. Grabolle, T. Neisius, W. Meyer-Klaucke, H. Dau, Biochemistry **44**, 1894–1908 (2005)
57. M. Lundberg, M.R.A. Blomberg, P.E.M. Siegbahn, Theor. Chem. Acc. **110**, 130–143 (2003)
58. E.M. Sproviero, K. Shinopoulos, J.A. Gascon, J.P. McEvoy, G.W. Brudvig, V.S. Batista, Philos. Trans. R. Soc. Lond. B **363**, 1149–1156 (2008)
59. R. Tagore, R.H. Crabtree, G.W. Brudvig, Inorg. Chem. **46**, 2193–2203 (2007)
60. R. Tagore, H.Y. Chen, R.H. Crabtree, G.W. Brudvig, J. Am. Chem. Soc. **128**, 9457–9465 (2006)
61. S. Zein, L.V. Kulik, J. Yano, J. Kern, Y. Pushkar, A. Zouni, V.K. Yachandra, W. Lubitz, F. Neese, J. Messinger, Philos. Trans. R. Soc. Lond. B **363**, 1167–1177 (2008)